Catena 170 (2018) 290–304

Contents lists available at ScienceDirect

Catena

journal homepage: www.elsevier.com/locate/catena

Effect of temperature on soil structural stability as characterized by high energy moisture characteristic method

H. Kelishadi[a], M.R. Mosaddeghi[a,*], S. Ayoubi[a], A.I. Mamedov[b,c]

[a] Department of Soil Science, College of Agriculture, Isfahan University of Technology, Isfahan 84156-83111, Iran
[b] Faculty of Agriculture, Arid Land Research Center, Tottori University, Tottori 680-0001, Japan
[c] Institute of Botany, Azerbaijan National Academy of Sciences (ANAS), AZ1073 Baku, Azerbaijan

ARTICLE INFO

Keywords:
Soil structural stability
Temperature
High energy moisture characteristic
Calcareous soils
Air entrapment
Pore size distribution

ABSTRACT

Temperature is a key factor that can affect soil properties and processes. Surface tension-viscous flow (STVF) theory is widely used to explain the temperature effects on soil hydraulic properties. We hypothesized that one of the reasons for deviation of measured soil water retention data from the STVF theory predictions is due to the temperature effects on soil structural stability (i.e., near-saturated pore size distribution [PSD]). Therefore, the objective of this study was to evaluate the effect of temperature on soil structural stability as characterized using the high energy moisture characteristic (HEMC) method in a wide range of arid and semi-arid soils of Iran. Aggregates of 28 soil samples were fast-wetted to mimic the natural conditions of soils during rainfall and irrigation. Four ambient temperatures (5, 10, 15 and 30 °C) were applied using an incubator during the wetting of aggregates, and after that HEMCs in the matric suction (h) range of 2 to 50 hPa were measured. Both van Genuchten (VG) and modified van Genuchten (MVG) models were fitted to the HEMC data and structural stability indices were calculated. The results generally showed that ambient temperature significantly altered soil PSD and structural stability, and as temperature increased: (i) an expansion of entrapped air initiated by the formation of microbubbles, was enhanced, (ii) water content at near full saturation $h = 2$ hPa ($\theta_{2\text{hPa}}$) decreased, and at $h = 50$ hPa ($\theta_{50\text{hPa}}$) it increased, leading to a reduction in the volume of drainable pores [VDP], and thus (iii) the soil structural index [SI] and slope at the inflection point of HEMC [S_i] decreased, and (iv) amount of macropores (h, 2–12 hPa) was markedly decreased, however, micropores (h, 12–50 hPa) were not notably affected or were increased at high temperature due to intensive shifting of macropores into micropores. These findings imply that soil structure was damaged due to loosening effects of high temperatures on inter-particles bonds and increased repulsive forces between clay particles. Cluster analysis showed that the effect of ambient temperature on the structural stability was greatest in carbonate-rich soils with low clay and organic carbon (OC) contents and was least in the soils rich in OC. The results of this study could be important for projecting the effect of global warming and climate change on soil structure and erosion.

1. Introduction

Soil structure is described by the arrangement of primary particles into secondary components, which are called aggregates. Structural stability is the capability of soil to hold solid and pore space architecture when exposed to external stresses (i.e., tillage, irrigation, cropping, compaction, climate, etc.). Structure is a key property of soils which can affect different processes (i.e., water retention, infiltration, runoff generation, and soil erosion) in the soil and environment and largely used to evaluate soil quality and susceptibility to runoff and erosion (Dexter, 1988; Amezketa, 1999; Barthès and Roose, 2002; Mamedov and Levy, 2013).

Temperature is a key factor in the context of climate that may affect soil functioning and physical quality. The effect of temperature on soil hydraulic conductivity, infiltration (Constantz, 1982; Levy et al., 1989), water retention (Romero et al., 2001; Bachmann et al., 2002; Jacinto et al., 2009), and runoff and erosion (Ariathurai and Arulanandan, 1978; Ronan et al., 1998; Sachs and Pariente, 2017) have been reported in numerous studies, although many complexities and ambiguities in the interpretation of data still remain. Surface tension-viscous flow theory (STVF theory) is widely used as an acceptable concept to explain the temperature effects on soil hydraulic properties. The response of soil hydraulic properties to the variation of temperature due soil surface modifications can be explained by change in surface tension and

* Corresponding author.
E-mail address: mosaddeghi@cc.iut.ac.ir (M.R. Mosaddeghi).

https://doi.org/10.1016/j.catena.2018.06.015
Received 13 June 2017; Received in revised form 2 June 2018; Accepted 17 June 2018

viscosity of water in this theory (Philip and de Vries, 1957). However, the results of Jacinto et al. (2009) showed that the soil water retention capacity decreased with temperature, greater than that predicted by the change in surface tension, especially at high temperatures and low matric suctions. Experimental data by Haridasan and Jensen (1972), She and Sleep (1998) and Bachmann et al. (2002) revealed that decrease in matric suction due to an increase in temperature was considerably greater than the rate which is predicted using the STVF theory of Philip and de Vries (1957). Grant and Bachmann (2002) proposed four mechnisms to explain greater dependency of matric suction to temperature than that predicted by Philip and de Vries (1957) theory as follows: 1) increases of entrapped-air with an increase in temperature, 2) water expansion due to an increase in temperature, 3) the effect of temperature-mediated solute concentration on surface tension of the soil water, and 4) the sensitivity of soil-water contact angle to temperature. Although these mechanisms were closely linked to the effect of temperature on soil hydraulic properties, they could not completely explain the results associated with intricate interaction of soil properties and conditions (e.g., Gao and Shao, 2015).

Climate parameters might considerably affect structural condition and aggregate stability of soils from semi-arid and arid regions. Romero et al. (2001) suggested that the mechanisms for the effect of temperature (in the range 22–80 °C) on water retention of Boom clay (with mixed clay mineralogy) are different for the two intra- and inter-aggregate pore spaces. The water held in the inter-aggregate pore space is controlled by the capillary forces. In this region, the effects of temperature are mainly associated with temperature dependence of surface tension and soil-water contact angle, thermal expansion of entrapped air, and dissolved air release upon heating or surface tension change caused by dilation of water. In the second region, water is held in the small pores inside the aggregates where the soil water retention characteristic would mainly depend on clay microstructure and water flow chemistry through the pores (Romero et al., 2001). van der Drift (1995) reported that the variation of temperature did not have significant effect on soil aggregate stability. However, Lavee et al. (1996) reported that seasonal dynamics of aggregate stability was controlled by soil temperature and moisture in arid and Mediterranean climate conditions. Dimoyiannis (2009) also found that rainfall and temperature are the dominant factors affecting seasonal variation of soil aggregate stability. Ambient temperature is also important in hydrology and soil erosion. In the experiment of Sachs and Pariente (2017), soil loss (e.g., erosion) increased from 5 to 18 g m^{-2} with an increase in the temperature difference between rainfall and soil surface (i.e., with an increase in rainfall temperature from 20 to 35 °C). Authors concluded that thermophoresis due to thermal gradients in the soil solution decreased the stability of aggregates and hence increased the soil losses. Ariathurai and Arulanandan (1978) mentioned that increasing soil temperature might reduce the mutual attraction between clay particles, and as expected, the erosion rate would increase with increasing temperature while critical shear stress would decrease in a similar manner.

We hypothesized that (i) one of the reasons for deviation of measured soil water retention data from the predictions of Philip and de Vries (1957) theory is due to the temperature effects on soil structural stability (macroporosity), (ii) soil structure stability can be affected by an increase in entrapped-air and its expansion due to an increase in temperature, and (iii) changes in temperature would also affect the rate of wetting, and therefore, the temperature can indirectly affect aggregate stability as well. Increase in temperature might weaken the binding and cohesive forces between the particles and aggregates because temporal expansion coefficients would be different between the mineral particles and water, which can modify the pore (aggregate) geometry and size distribution. Moreover, entrapped air is believed to be responsible for the enhanced sensitivity to temperature of capillary pressure, and the volume of entrapped air increases with temperature, but they have not been supported by the experiment (Peck, 1960). According to the Young-Laplace equation, soil matric suction is dependent on soil-water contact angle, which would depend on temperature.

Several methods are available to measure aggregate stability but no unique method and/or procedure has been suggested yet for all soils (Le Bissonnais, 1996), since selection of the method and interpretation of the results would mostly depend on the aim of a study (Saygın et al., 2012; Pulido Moncada et al., 2015). High energy moisture characteristic (HEMC) method has been used for monitoring widely varying stability of soil structure, and adequately sensitive to distinguish small changes in aggregate and structure stability due to changes in soil properties, conditions and agricultural managements (Pierson and Mulla, 1989; Mamedov et al., 2010, 2014, 2017; Hosseini et al., 2015, 2017). In this method, the aggregate stability against precisely controlled wetting stresses is determined and its structural stability indices are related to pore size distribution (PSD). Dexter (2004) introduced the *S*-theory based on the conceptual relation between soil structure and PSD derived from the soil water characteristic curve. The slope of soil water characteristic curve at the inflection point [i.e., $S = \mathrm{d}\theta/\mathrm{d}(\ln h)$] was considered as an indicator of soil physical quality. Recently, Hosseini et al. (2015) adapted this theory for the HEMC method and introduced the slope of HEMC (in the h range of 0–50 hPa) at the inflection point ($S_i = \mathrm{d}\theta/\mathrm{d}h$) instead of S. The value of S_i represents the extent to which the aggregate porosity is concentrated into a narrow range of pore sizes. They found a positive and significant relationship between the stability indices of the original HEMC theory and the S_i, confirming the suitability of the new relative stability index (Hosseini et al., 2015).

To the best of our knowledge, no detailed quantitative investigation has been found in the literature about the effect of ambient temperature on soil structural stability. Therefore, the objective of this study was to quantitatively evaluate the effect of temperature on soil structural stability using the HEMC method in a wide range of semi-arid and arid region soils of Iran. The HEMC was also chosen to characterize the breakdown (e.g., slaking) of aggregates due to entrapped-air and hydration energy in temperature-dependent ways.

2. Materials and methods

2.1. Soil sampling and preparation

Soil samples with a vast range of physical and chemical properties were collected from the surface soils of 28 locations in Isfahan and Charamahal-va-Bakhtiari provinces, Iran, in August 2015. In each location, three soil samples from the same field were collected and mixed. The studied soils are mainly developed on carbonatic marl deposits of the Mesozoic Era, Cretaceous period (66–138 million years ago). The clay minerals of the studied soils are a mixture of smectites, kaolinite, illite, chlorite and vermiculite (Khademi and Mermut, 1998; Noruzi Fard et al., 2010). The major land uses are pasture, dryland and irrigated farming (Table 1).

Soil samples were carefully collected, air-dried and gently sieved to separate 0.5–1.0 mm intact aggregates for structural stability determination using the HEMC method. This size range of aggregates was separated because it was the predominant fraction (> 50%) of macroaggregates in the soils. In the studied soils, the aggregates in the 0.5–1 mm fraction were on average 89% (in the range 100–63%) and sand particles in the 0.5–1 mm fraction are on average 11% (in the range 0–37%). Therefore, the aggregates were predominant in the 0.5–1 mm fraction in the studied soils. In fact for comparing the effect of treatments (e.g., temperature in our study) on soil structural stability indices, it is not possible and/or important to separate intact aggregates of a size range from the sand particles of the same size range for the HEMC test (Mamedov and Levy, 2013). Moreover, the stability of aggregates in a fraction (i.e., 0.5–1 mm) is compared because the sand particles are not notably affected by the treatments (e.g., temperature). This assumption is also valid in all of the studies using the HEMC

Table 1
Physical and chemical properties of the studied soils.[a]

Soil no.	OC	CCE	Sand (0.05–2 mm)	Silt (0.002–0.05 mm)	Clay (< 0.002 mm)	Textural class	Land use	Cluster no.
	kg 100 kg^{-1}							
1	1.01	47.3	6.5	65.2	28.3	Silty clay loam	IF	3
2	0.22	47.0	51.2	34.5	14.2	Loam	P	4
3	0.74	32.5	23.7	48.0	28.3	Clay loam	IF	2
4	1.68	35.0	28.1	54.0	17.9	Silt loam	P	2
5	0.75	10.8	5.5	59.6	35.0	Silty clay loam	DF	1
6	0.78	18.0	11.3	61.2	27.6	Silty clay loam	P	1
7	0.57	56.0	26.7	53.9	19.4	Silt loam	P	4
8	1.11	16.5	21.0	58.1	20.9	Silt loam	P	1
9	0.08	63.3	49.2	39.5	11.3	Loam	P	4
10	0.99	32.5	6.8	62.6	30.5	Silty clay loam	IF	3
11	0.18	31.0	9.0	59.7	31.3	Silty clay loam	DF	3
12	0.55	12.7	10.3	62.9	26.8	Silt loam	P	1
13	0.41	48.3	14.5	56.5	29.0	Silty clay loam	P	3
14	2.37	33.5	19.1	62.9	18.0	Silt loam	P	2
15	0.69	32.0	22.6	59.4	17.9	Silt loam	P	2
16	3.88	46.3	6.6	69.5	23.9	Silt loam	P	3
17	0.59	33.0	10.1	56.5	33.5	Silty clay loam	P	3
18	0.90	50.2	37.5	49.8	12.8	Loam	P	4
19	0.78	42.5	1.4	74.0	24.6	Silt loam	IF	3
20	0.33	55.3	29.3	51.3	19.4	Silt loam	P	4
21	0.33	29.8	6.6	62.1	31.3	Silty clay loam	P	3
22	8.88	37.0	1.8	64.0	34.2	Silty clay loam	P	3
23	0.67	31.0	11.7	63.7	24.6	Silt loam	P	3
24	0.58	23.5	21.9	53.5	24.6	Silt loam	IF	2
25	0.50	20.0	18.9	59.5	21.6	Silt loam	P	1
26	0.76	43.3	25.2	53.2	21.6	Silt loam	IF	2
27	1.92	37.5	8.0	62.2	29.8	Silty clay loam	IF	3
28	0.49	51.3	8.8	62.9	28.3	Silty clay loam	P	3
Max	8.88	63.2	51.2	74.0	35.0			
Min	0.078	10.7	1.4	34.59	11.3			
Mean	1.17	36.3	17.6	57.9	24.5			
CV	145.3	37.4	74.0	14.3	26.6			

[a] OC: organic carbon, CCE: calcium carbonate equivalent, CV: coefficient of variation, IF: irrigated farming, DF: dryland farming, P: pasture.

method for soil structural stability assessment (Mamedov and Levy, 2013). A part of the soil was ground and passed through a 2-mm sieve for measurement of routine soil properties. Soil texture was determined using the pipette method (Gee and Bauder, 1986), organic carbon (OC) by the wet-oxidation method (Nelson and Sommers, 1986) and calcium carbonate equivalent (CCE) using the back-titration with NaOH (Nelson, 1982).

2.2. The HEMC theory

The HEMC method for assessing the structural stability was first proposed by Childs (1940). Collis-George and Figueroa (1984), Pierson and Mulla (1989), and finally Levy and Mamedov (2002) modified the method to quantify and standardize the experimental procedure and modeling approach. According to the modified method, two separate batches of aggregates are wetted either slowly or quickly and their water characteristic curves at high energies (i.e. low matric suctions) are measured. An index of structural stability is obtained by quantifying the differences in HEMCs for the pre-wetted aggregates. A structural index (SI) is defined as the ratio of volume of drainable pores (VDP) to modal suction (h_{modal}). The ratio of fast to slow SI values, termed stability ratio (SR), is used to compare stability of aggregates on a relative scale of 0 to 1 (Collis-George and Figueroa, 1984; Pierson and Mulla, 1989; Levy and Mamedov, 2002; Mamedov and Levy, 2013), but for the given treatments only SI for the fast wetting rate is widely used too (Mamedov et al., 2017).

2.3. Aggregates preparation, temperature treatments and HEMC determination

Ten grams of the 0.5–1.0 mm intact aggregates were poured into PVC cylinders (2.8 cm diameter and 3 cm height) to form a 15 mm-thick bed. Soil aggregates were only wetted at a fast rate by rapid wetting with distilled water before HEMC determination to mimic the natural conditions of soils during rainfall and irrigation with low concentration of salts. Fast wetting also applies stresses due to entrapped air and non-even swelling to the aggregates; therefore, the effect of temperature on structural stability could be better quantified by its data.

Four ambient temperatures (5, 10, 15 and 30 °C) were applied using an incubator during the fast wetting. The applied temperature was controlled using a thermometer inside the incubator. The selected temperatures cover the range of air temperatures in the studied regions when rainfall happens, and the temperatures in the laboratory when routine soil measurements are done. The prepared aggregates were submerged and kept in the distilled water with the predefined temperature for 24 h (Poch and Antunez, 2010) to obtain full equilibrium condition when the temperatures of water and aggregates were the same for each treatment. In total, 112 batches of aggregates (i.e., 28 soils × 4 ambient temperatures) were prepared and studied.

The HEMCs of the fast-wetted aggregates were determined at different soil matric suctions (h) in the range of 2 to 50 hPa (with a small increment of 2–3 hPa) using a sandbox (Eijkelkamp, Giesbeek, The Netherlands) at the laboratory temperature (≈22 °C). Samples were weighed after they equilibrated at each h. Finally all samples were oven-dried and weighed such that the values of gravimetric water content (θ, g g^{-1}) were calculated as a function of h (Mamedov and Levy, 2013; Hosseini et al., 2015, 2017).

2.4. HEMC modeling and calculation of structural stability indices

Hosseini et al. (2015) reported significant correlations between model parameters and structural indices between the van Genuchten

(VG) and modified van Genuchten (MVG) models and hence both models were fitted to the measured HEMC data in the h range of 2–50 hPa to determine the structural stability indices (Pierson and Mulla, 1989; Levy and Mamedov, 2002; Mamedov and Levy, 2013; Hosseini et al., 2015):

$$\theta(h) = \theta_r + (\theta_s - \theta_r)[1 + (\alpha h)^n]^{\left(\frac{1}{n}-1\right)} \quad (1)$$

$$\theta(h) = \theta_r + (\theta_s\text{-}\theta_r)[1 + (\alpha h)^n]^{\left(\frac{1}{n}-1\right)} + Ah^2 + Bh + C \quad (2)$$

where θ_r and θ_s are *pseudo* residual and saturated water contents ($g\,g^{-1}$) that cannot be physically interpreted in terms of saturated and residual water contents (Pierson and Mulla, 1989). The α (hPa^{-1}) and n ($-$) are the empirical parameters which control position and steepness of the water retention curve, respectively; A (hPa^{-2}), B (hPa^{-1}), and C ($g\,g^{-1}$) are the quadratic coefficients (Pierson and Mulla, 1989) to improve model fitting to the measured data. Eq. (2) was used because the original van Genuchten (1980) model accurately estimates h_{modal}, but does not provide an accurate estimation of VDP. Pierson and Mulla (1989) showed that this modification has little effect on the values of parameters n and α, but it significantly affects the values of θ_r and θ_s, so that the model will accurately fit the legs of the HEMC data. The parameters were derived by fitting Eqs. (1) and (2) to the measured HEMC data using the non-linear optimization technique of Solver Tool (Wraith and Or, 1998) in Microsoft Excel® (Microsoft Corporation, Redmond, Washington State, US).

The specific water capacity function [$C(\theta) = |d\theta/dh|$, hPa^{-1}] was computed as the first derivative of Eqs. (1) and (2) using Eqs. (3) and (4):

$$C(\theta) = |d\theta/dh| = (\theta_s\text{-}\theta_r)[1 + (\alpha h)^n]^{\left(\frac{1}{n}\text{-}1\right)}(\alpha h)^n(n/\{h[1 + (\alpha h)^n]\}) \quad (3)$$

$$C(\theta) = |d\theta/dh| = (\theta_s\text{-}\theta_r)[1 + (\alpha h)n]^{\left(\frac{1}{n}-1\right)}\left(\frac{1}{n} - 1\right)(\alpha h)^n\left((n/\{h[1 + (\alpha h)^n]\}) + 2Ah + B\right. \quad (4)$$

The VDP_{MVG} ($g\,g^{-1}$) values were calculated by finding the area bound by the pore shrinkage line (i.e., $2Ah + B$) and the specific water capacity curve, Eq. (4), using trapezoidal numerical integration. The pore shrinkage baseline represents the rate of water loss due to aggregate shrinkage rather than pore emptying. The VDP_{MVG} is theoretically equal to $(\theta_s - \theta_r)$ as revealed in the data presented by Pierson and Mulla (1989). The VDP_{VG} determined as area bound by $C(\theta)$ function, Eq. (3), and the x-axis (i.e., h) in the h range of 2 to 50 hPa, and it was calculated using trapezoidal numerical integration as follows:

$$VDP_{VG} = \sum_{i=1}^{k} (h_i + h_{i+1}) \times \left(\frac{C(\theta_i) + C(\theta_{i+1})}{2}\right) \quad (5)$$

where k is the number of intervals in the given matric suction range (i.e., 2–50 hPa), h_i and h_{i+1} are two successive matric suctions, and $C(\theta_i)$ and $C(\theta_{i+1})$ are the values of specific water capacity, Eq. (3), at corresponding successive h or θ values, respectively.

The modal suctions (h_{modal} and h_i, hPa) for Eqs. (1) or (2) were calculated by the following equation (Hosseini et al., 2015):

$$h_{modal} \approx \frac{1}{\alpha}\left(\frac{n-1}{n}\right)^{1/n} \quad (6)$$

A structural index (SI, hPa^{-1}) was defined as the ratio of VDP_{MVG} to h_{modal} (Collis-George and Figueroa, 1984; Pierson and Mulla, 1989):

$$SI = \frac{VDP_{MVG}}{h_{modal}} \quad (7)$$

The absolute value of the slope at the inflection point of HEMC, an index of structural stability (S_i, hPa^{-1}), is obtained by the following equation (Hosseini et al., 2015):

$$S_i = |d\theta/dh| = (\theta_s - \theta_r) \times n\alpha \times \left(\frac{n-1}{2n-1}\right)^{\left(\frac{2n-1}{n}\right)} \quad (8)$$

Different structural stability indices including SI, VDP_{MVG}, h_{modal}, S_i, h_i and VDP_{VG} were calculated. In order to quantify the effect of temperature on PSD, the calculated VDP values of both models (i.e., VG and MVG) were also divided into two groups of pores at the h ranges of 2–12 hPa and 12–50 hPa which were conditionally considered as "macropores (1500–250 μm)" and "micropores (250–60 μm)" (i.e., contribution of large and small aggregates to VDP) within the studied range of (macro)pores (2–50 hPa) named $VDP_{VG\text{-}macro}$ or $VDP_{MVG\text{-}macro}$ and $VDP_{VG\text{-}micro}$ or $VDP_{MVG\text{-}micro}$, respectively (Soil Science Society of America, 1997; Mamedov and Levy, 2013). Measured water contents at first and last h values of 2 and 50 hPa (θ_{2hPa} and θ_{50hPa}) and the total soil water released in the mentioned h range ($\Delta\theta_{2–50}$) were also considered for analyzing the effect of temperature on soil structural stability. The $\Delta\theta_{2–50}$ is comparable with the VDP, but the measured data were analyzed directly in order to avoid the errors during HEMC data modeling.

2.5. Statistical analysis

Complete randomized block design was used to statistically compare the effect of ambient temperature on soil structural stability indices (i.e., SI, VDP_{MVG}, h_{modal}, S_i, h_i and VDP_{VG}, $VDP_{VG\text{-}macro}$, $VDP_{MVG\text{-}macro}$, $VDP_{VG\text{-}micro}$, $VDP_{MVG\text{-}micro}$, θ_{2hPa}, θ_{50hPa} and $\Delta\theta_{2–50}$). Ambient temperature and soil type were considered as treatment and block (replicate), respectively. Mean comparisons were done using least significant difference (LSD) test ($P < 0.05$). Correlation analysis was also done for interpretation of the results. Data were analyzed using SAS software (SAS Institute, 2008).

For better interpretation of the data, the studied soils were clustered based on sand, silt, clay, OC and CCE contents by K-means test using MATLAB v. 14 software (Mathworks, Inc., Natick, MA, USA). The K-means clustering finds a partition in which objects within each cluster are as close to each other as possible, and as far from objects in other clusters as possible. Each cluster in the partition is defined by its member objects and by its centroid, or center. The centroid for each cluster is the point to which the sum of distances from all objects in that cluster is minimized. The K-means computes cluster centroids differently for each distance measure, in order to minimize the sum with respect to the measure that a researcher specifies (Mathworks, Inc., Natick, MA, USA).

Finally, a complete randomized block design was employed to analyze the HEMC data and indices after clustering. The mean comparisons were done using the LSD test to quantify the effect of temperature on the structural stability indices in different clusters. Figures were drawn using SigmaPlot (Systat Software, San Jose, CA) and Microsoft Excel® (Microsoft Corporation, Redmond, Washington State, US).

3. Results and discussion

3.1. Soils description

Physical and chemical properties of the studied soils are given in Table 1. Soils were generally highly calcareous (CCE in the range of 10.7–63.2 kg 100 kg^{-1}, mostly > 20 kg 100 kg^{-1}) with a vast range of different properties (Table 1) and representative of arid and semi-arid calcareous soils in central Iran. The coefficient of variation (CV) of measured soil properties indicated that soils have broad ranges of the intrinsic properties especially for the OC content (0.08–8.88 kg 100 kg^{-1}, but mostly < 2.00 kg 100 kg^{-1}) and texture (from silt loam to silty clay loam). This allowed us to evaluate the effect of ambient temperature on structural stability in a good range of semi-arid and arid region calcareous soils.

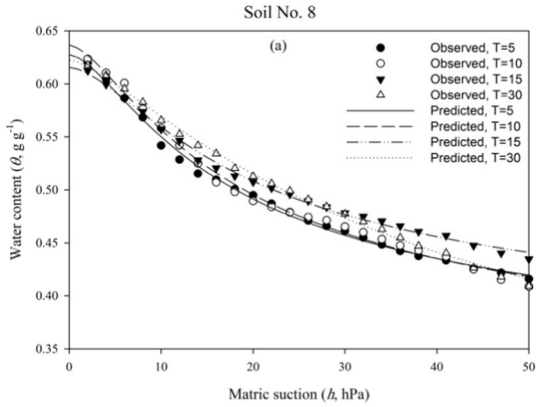

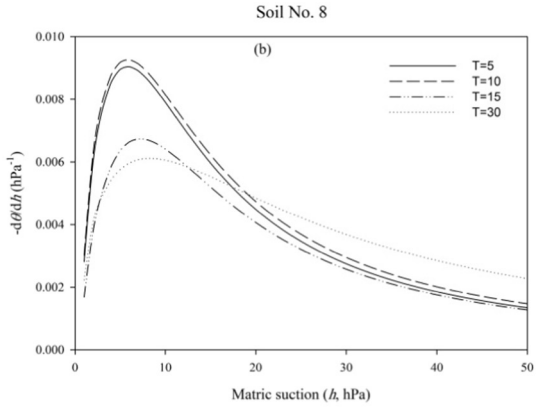

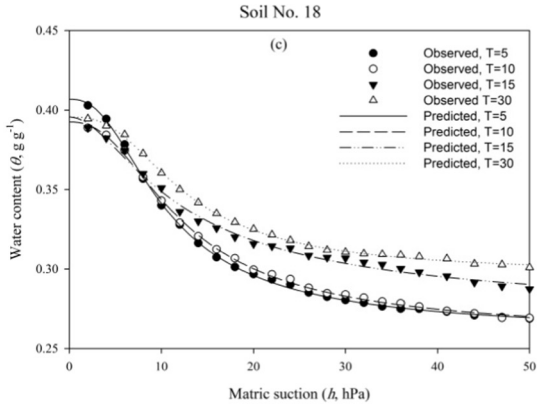

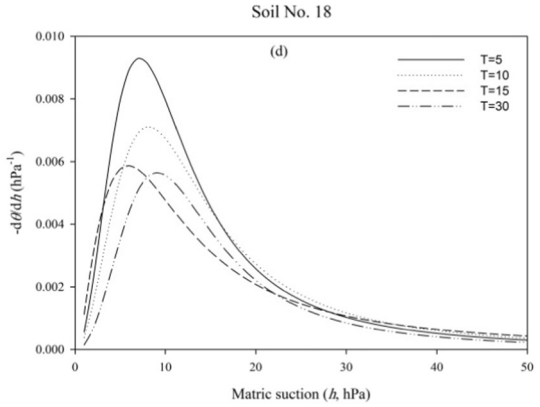

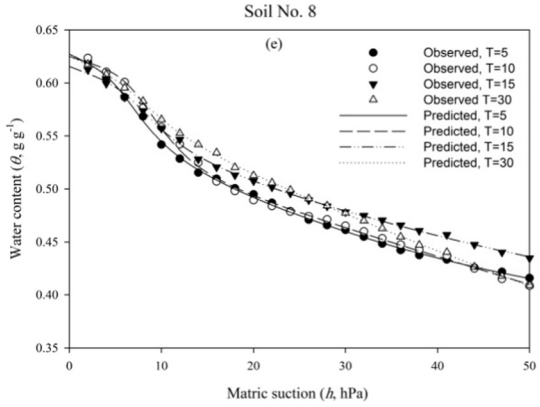

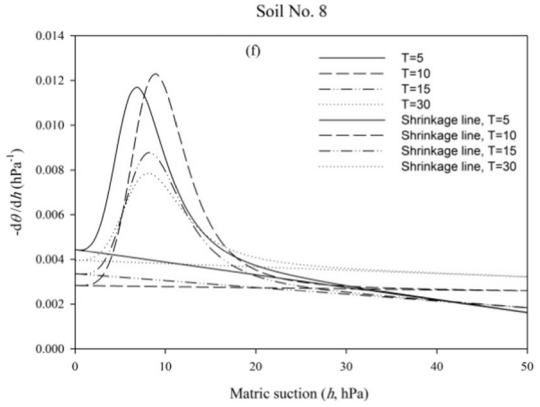

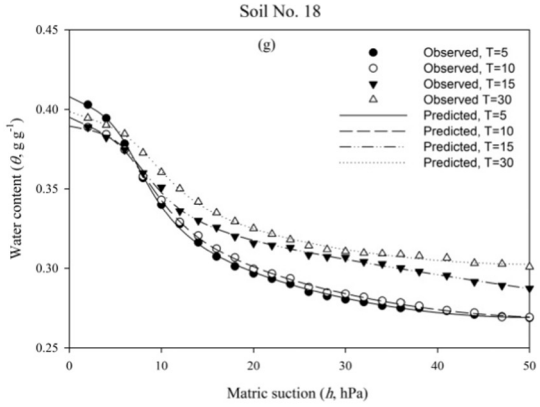

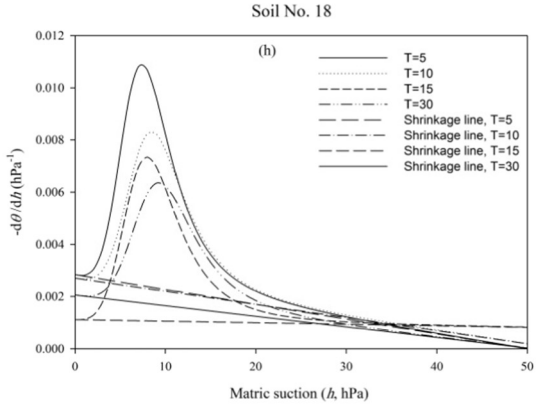

(caption on next page)

Fig. 1. Examples of high energy moisture characteristics (HEMC) and corresponding specific water capacity ($|d\theta/dh|$) curves of two soils (No. 8 and 18), as affected by ambient temperature: (a and c) measured and predicted HEMCs by the original van Genuchten model, (b and d) corresponding specific water capacity ($|d\theta/dh|$) curves for (a) and (c), (e and g) measured and predicted HEMCs by the modified van Genuchten model, and (f and h) corresponding specific water capacity ($|d\theta/dh|$) curves for (e) and (g).

3.2. Effect of ambient temperature on HEMC curves and soil water retention

Analysis of variance (ANOVA) showed that the soil water retention and structural stability indices were significantly affected by block (soil) and ambient temperature (data not shown). The effect of soil type on all the studied parameters was significant at $P < 0.001$, indicating that the studied soils were different in terms of HEMC and its parameters and indices. Moreover, the effect of temperature on the majority of the parameters and indices was also significant at $P < 0.001$. The effects of temperature on $VDP_{MVG\text{-}macro}$ and SI were significant at $P < 0.01$ and $P < 0.05$, respectively. However, the temperature did not have significant effect on h_i, VDP_{MVG} and h_{modal}.

Examples of HEMC and specific water capacity [$C(\theta) = |d\theta/dh|$] curves in the fast-wetted aggregates as affected by ambient temperature are shown in Fig. 1. The selected soils, silt loam and loam (No. 8 and 18 accordingly, see Table 1) were allocated in clusters 1 and 3, respectively (see Table 4), and responded differently to temperature. The SI of soil No. 8 with 20.9 kg 100 kg^{-1} clay had an irregular trend with temperature while the SI of soil No. 18 with 12.8 kg 100 kg^{-1} clay had a regular trend with temperature. Corresponding values of fitting parameters of the modified and original van Genuchten models used for the examples of Fig. 1, are presented in Table 2. Results (Fig. 1 and Table 2) indicated that (i) the fit of the modified and original van Genuchten models to the various HEMC data was excellent ($R^2 > 0.99$), and (ii) the shape and steepness of the soil water retention curves and hence the structural stability indices were considerably affected by the temperature. However, the effect of temperature on the HEMC would depend on the intrinsic properties of the soils. The water retention data of the aggregates exposed to low temperatures were higher and lower than those exposed to high temperatures in the ranges of h from 2 to 10–12 hPa (pore size > 250–300 μm) and 10–12 to 50 hPa (pore size < 250–300 μm), respectively, being more evident in the weakly-structured soil (Fig. 1). This finding may be attributed to lower degree of slaking and higher stability of the soil aggregates at low temperatures.

Mamedov and Levy (2013) divided HEMCs (on the basis of critical points of the S-shaped water retention curves of 0.5–1.0 mm size aggregates) into two subclasses of the macropores > 250 μm (i.e., in the h range of 0–12 hPa) and the micropores 250–60 μm (i.e., in the h range of 12–50 hPa). Using these subclasses assisted us to understand what macropore sizes, and hence apparent macro-aggregate sizes, were affected by the treatments. At the h range 2 to 40 hPa (pore size > 75 μm), the samples treated with low temperature had higher water contents and more stable structure (i.e., greater VDP) than the samples treated with high temperature (Fig. 1 and Table 2). Similarly, Hosseini et al. (2015) reported that rhizosphere soils of tall fescue had higher water contents (especially near the saturation zone) and VDP values for the fast-wetted aggregates, which was attributed to more stable aggregates in the rhizosphere.

Measured water contents at first and last h values of 2 and 50 hPa (θ_{2hPa} and θ_{50hPa}) and the total soil water released in the mentioned h range ($\Delta\theta_{2-50}$) were also analyzed. Generally θ_{2hPa} significantly decreased as temperature increased and hence, maximum and minimum values of θ_{2hPa} were observed at temperatures of 5 and 30 °C, respectively (Fig. 2a). However, θ_{50hPa} significantly increased with an increase in the temperature (Fig. 2b), revealing that frequency of small

Table 2
Fitting parameters of the modified van Genuchten (MVG) model [Eq. (2)] and original van Genuchten (VG) model [Eq. (1)] and structural stability indices for soil examples (No. 8 and 18) at the ambient temperatures of 5, 10, 15 and 30 °C.[a]

Soil no.	Fitting parameters	MVG model				VG model			
		5	10	15	30	5	10	15	30
Soil no. 8	θ_r (g g^{-1})	0.398	0.381	0.380	0.411	0.303	0.284	0.336	0.080
	θ_s (g g^{-1})	0.458	0.461	0.430	0.449	0.628	0.637	0.615	0.623
	α (hPa^{-1})	0.136	0.107	0.114	0.115	0.104	0.101	0.085	0.054
	n (−)	4.09	4.82	4.35	4.12	1.61	1.58	1.65	1.42
	A (hPa^{-2})	0.000028	0.000002	0.000015	0.000007	–	–	–	–
	B (hPa^{-1})	−0.0044	−0.0028	−0.0034	−0.0040	–	–	–	–
	C (g g^{-1})	0.169	0.164	0.185	0.176	–	–	–	–
	VDP (g g^{-1})	0.060	0.079	0.050	0.037	0.207	0.218	0.174	0.206
	h_{modal} or h_i (hPa)	6.86	8.89	8.28	8.15	5.27	5.26	6.69	7.76
	SI or S_i (hPa^{-1})	0.0088	0.0089	0.0060	0.0045	0.0091	0.0093	0.0068	0.0061
	$\theta_{r\text{-}observed}$ (g g^{-1})	0.416	0.409	0.435	0.409	0.416	0.409	0.435	0.409
	$\theta_{s\text{-}observed}$ (g g^{-1})	0.728	0.737	0.705	0.695	0.728	0.737	0.705	0.695
	R^2	0.999	0.998	0.998	0.999	0.997	0.995	0.997	0.997
Soil no. 18	θ_r (g g^{-1})	0.187	0.192	0.188	0.187	0.260	0.258	0.267	0.300
	θ_s (g g^{-1})	0.255	0.245	0.241	0.255	0.407	0.393	0.396	0.396
	α (hPa^{-1})	0.127	0.111	0.118	0.127	0.123	0.106	0.127	0.099
	n (−)	4.31	4.46	4.31	4.31	2.48	2.43	1.91	2.72
	A (hPa^{-2})	0.000028	0.000025	0.000003	0.000028	–	–	–	–
	B (hPa^{-1})	−0.0028	−0.0027	−0.0011	−0.0028	–	–	–	–
	C (g g^{-1})	0.153	0.150	0.148	0.153	–	–	–	–
	VDP (g g^{-1})	0.068	0.053	0.054	0.044	0.137	0.122	0.105	0.093
	h_{modal} or h_i (hPa)	7.43	8.54	7.97	9.35	6.59	7.59	5.34	8.55
	SI or S_i (hPa^{-1})	0.0091	0.0062	0.0067	0.0047	0.0094	0.0071	0.0059	0.0057
	$\theta_{r\text{-}observed}$ (g g^{-1})	0.269	0.269	0.287	0.269	0.269	0.269	0.287	0.269
	$\theta_{s\text{-}observed}$ (g g^{-1})	0.524	0.513	0.485	0.524	0.524	0.513	0.485	0.524
	R^2	0.999	0.999	0.998	0.998	0.999	0.999	0.997	0.999

[a] θ_r and θ_s: the *pseudo* residual and saturated water contents, respectively, α and n: the fitting parameters which control position and steepness of HEMC, respectively; and A, B, and C: the quadratic fitting coefficients. $\theta_{s\text{-}observed}$ and $\theta_{r\text{-}observed}$: water contents measured at h values of 2 and 50 hPa, respectively, VDP: volume of drainable pores, h_{modal}: modal suction, SI: structural index, h_i and S_i: matric suction and slope at the inflection point of HEMC, respectively.

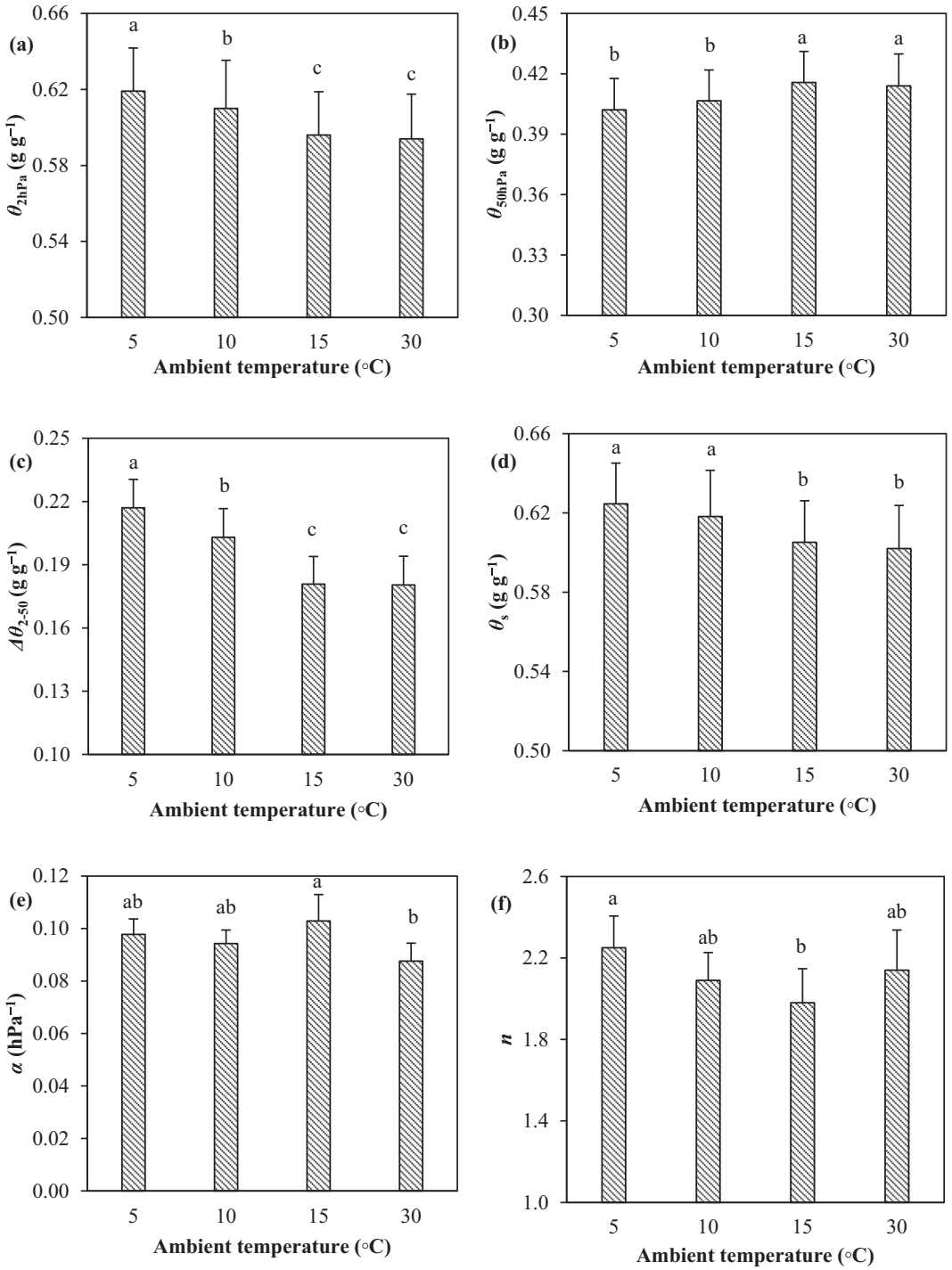

Fig. 2. Mean comparisons of the effect of ambient temperature on: (a and b) measured water contents at matric suctions (h) of 2 and 50 hPa (θ_{2hPa} and θ_{50hPa}), and (c) the total soil water released in the mentioned h range ($\Delta\theta_{2-50}$), and (d) saturated water content (θ_s), (e) scaling (α), and (f) shape (n) parameters of the original van Genuchten model. For each index, columns labeled with different letters are significantly different at $P < 0.05$ (LSD); Standard errors are shown on the bars.

pores increased at higher temperatures. As the temperature increased, $\Delta\theta_{2-50}$ significantly decreased (Fig. 2c). The decrease of θ_{2hPa} and increase of θ_{50hPa} with increasing the temperature clearly showed the collapse of soil pore space (e.g., aggregate breakdown) and destruction of macropores into smaller pores. The decreasing trend of $\Delta\theta_{2-50}$ with an increase in temperature also confirmed the reduction in VDP at high temperature.

3.3. Effect of ambient temperature on van Genuchten model parameters

The saturated water content (θ_s) predicted by the VG model significantly decreased with increase of ambient temperature (Fig. 2d). In the VG model, θ_s is considered approximately equal to measured saturated water content (i.e., total porosity). The decreases of θ_s with an increase in temperature confirmed that soil porosity decreased due to

destruction of pores. Demond and Roberts (1991) indicated that θ_s values increased as surface tension of soil pore water decreased and, in particular, found lower θ_s values for the air-water system compared to four lower surface tension organic-water systems. They pointed out that the factors affecting θ_s might be attributable to the changes in pendular moisture, PSD of the porous medium, and drainage rate of water from the porous medium. She and Sleep (1998) stressed that for the air-water system in silica sand, θ_s in the VG model was decreasing slightly when temperature increased from 20 to 60 °C, and significantly raised as temperature increased from 60 to 80 °C. The changes in PSD due to the changes in sand compaction with increasing temperature might happen because of the thermal expansion of the sand (She and Sleep, 1998).

The scaling parameter (α) relates to the inverse of matric suction at the inflection point of the soil water characteristic curve; a decrement in the α value shifts the curve towards higher h values meaning that the *desaturation zone* starts at higher values (Sillers et al., 2001). The α significantly decreased at temperature of 30 °C when compared with lower temperatures (Fig. 2e), indicating that the most frequent pore sizes are concentrated at higher h values with an increment in temperature. The parameter n governs the shape of the soil water characteristic curve in the desaturation zone (Sillers et al., 2001). The decreasing trend in n with the increase of temperature demonstrated that the slope of the desaturation zone would diminish at higher temperatures (Fig. 2f). Generally, several studies about the effect of different treatments and management practices on soil water characteristic curve indicated that changes in soil structure are reflected in n and α alteration (e.g., Asgarzadeh et al., 2010; Hosseini et al., 2016; Mamedov et al., 2017). However, we did not observe consistent and regular changes in n and α with temperature (Fig. 2e, f). The van Genuchten model and the parameters have usually been used for the whole range of h (i.e., 0–15,000 hPa) in conventional soil water characteristic curve analyses, and their applications and physical meanings need to be evaluated for HEMC data (i.e., low values of h) measured on a batch of aggregates; α and n represented contribution of macro-aggregates (> 0.25 mm) and micro-aggregates (< 0.25 mm) in some HEMC studies (Mamedov and Levy, 2013).

3.4. Effect of ambient temperature on soil structural stability indices and pore size fractions

Pearson's correlation analysis showed that the parameters and indices calculated using the van Genuchten model (i.e., VDP_{VG}, h_i and S_i) had positive and significant correlations with the corresponding values calculated using the modified van Genuchten model (i.e, VDP_{MVG}, h_{modal} and SI), respectively (Table 3). This finding implies that they could alternatively be used to characterize the soil structural stability in accordance with the results of Hosseini et al. (2015). Correlation between VDP_{macro} and VDP was significantly negative for both VG (−0.377) and MVG (−0.402) models (Table 3). However, when the data of three soils (numbers 14, 16 and 22) were excluded, the values of the correlation coefficient increased and became positive (i.e., 0.581 and 0.956 for the VG and MVG models, respectively), indicating that the total volume of drainable pores is primarily governed by the volume of the macropores in the studied soils. These three soils have greater organic matter content (> 2.4 kg 100 kg^{-1}) compared with the other soils (< 1–2 kg 100 kg^{-1}), and their VDP values were significantly higher. Presence of these soils in the correlation analysis would significantly affect the sign and value of the correlation coefficient because in spite of other soils, the h_i (or h_{modal}) values of these soils at all the temperatures were > 12 hPa (intermediate between micropores and macropores). This indicated that most water drainage in these three soils would occur at h values > 12 hPa (e.g., Demond and Roberts, 1991).

Clear trends of decreasing soil structural stability with ambient temperature were observed for the VDP_{VG} and S_i (Fig. 3a, b) and the VDP_{MVG} and SI (Fig. 3c, d).

Mean comparisons of the effects of temperature on VDP_{macro} and VDP_{micro} are presented in Fig. 4. The fractionation of total pore space into macropores and micropores illustrated that $VDP_{VG\text{-}macro}$ significantly decreased by an increase in the temperature (Fig. 4a). The same trend was also found for $VDP_{MVG\text{-}macro}$; however, the decreasing effect was only significant for the temperature of 30 °C (Fig. 4c). These findings imply the soil structure damage due to loosening effects of high temperatures on inter-particles bonds, which mainly destroyed the macropores (< 12 hPa). This finding might be explained by hierarchical organization of soil structural elements as suggested by Tisdall and Oades (1982) and Dexter (1988). They showed that humified/stable organic matter would stabilize micro-aggregates and incorporates in the micropores between the domains and clusters. However, newly-formed particulate organic matter contributing to macro-aggregates stability is sensitive to microbial decomposition and management practices. Therefore, stability of macro-aggregates is usually lower than micro-aggregates (Tisdall and Oades, 1982).

The $VDP_{VG\text{-}micro}$ and $VDP_{MVG\text{-}micro}$ significantly decreased by an increase in the temperature up to 15 °C and with an insignificant increase at 30 °C (Fig. 4b, d). The decreases in micropores with temperature up to 15 °C are not as much as those for the macropores on a relative basis (see Fig. 4a, c) indicating the higher susceptibility of soil macropores to temperature fluctuations. However, higher temperature (i.e., 30 °C) increased the VDP_{micro} perhaps due to intensive shifting of macropores into micropores associated also with slaking, due to an expansion of entrapped air (e.g., increasing formation of microbubbles).

The effect of temperature on soil structure stability might be governed by three major mechanisms: (i) change in soil-water contact angle (or wetting coefficient, cosine of the contact angle) and hydration rate, (ii) change in pore radius (r) by change in the Debye length as

Table 3
Pearson's correlation matrix between soil structural stability indices and pore fractions calculated by van Genuchten (VG) and modified van Genuchten (MVG) models in the studied soils.[a]

	VDP_{VG}	h_i	S_i	$VDP_{VG\text{-}macro}$	$VDP_{VG\text{-}micro}$	VDP_{MVG}	h_{modal}	SI	$VDP_{MVG\text{-}macro}$
h_i	0.790**	1							
S_i	0.832**	0.574**	1						
$VDP_{VG\text{-}macro}$	−0.377**	−0.771**	−0.223*	1					
$VDP_{VG\text{-}micro}$	0.964**	0.898**	0.775**	−0.611**	1				
VDP_{MVG}	0.802**	0.668**	0.929**	−0.467**	0.820**	1			
h_{modal}	0.824**	0.879**	0.645**	−0.636**	0.888**	0.726**	1		
SI	0.269**	−0.056^{ns}	0.651**	0.188^{ns}	0.176^{ns}	0.626**	0.034^{ns}	1	
$VDP_{MVG\text{-}macro}$	−0.618**	−0.834**	−0.333**	0.802**	−0.761**	−0.402**	−0.739**	0.372**	1
$VDP_{MVG\text{-}micro}$	0.862**	0.823**	0.872**	−0.649**	0.923**	0.953**	0.839**	0.390**	−0.660**

[a] h_i and S_i: matric suction and slope at the inflection point of HEMC respectively; h_{modal}: modal suction, SI: structural index, VG and MVG: related to the calculations using the van Genuchten and modified van Genuchten models, respectively; VDP: volume of drainable pores, and subscript *macro* and *micro* related to VDP values at the ranges of matric suction 2–12 and 12–50 hPa, respectively; ns, * and ** stand for non-significant, significant at 0.05 and 0.01 probability levels, respectively.

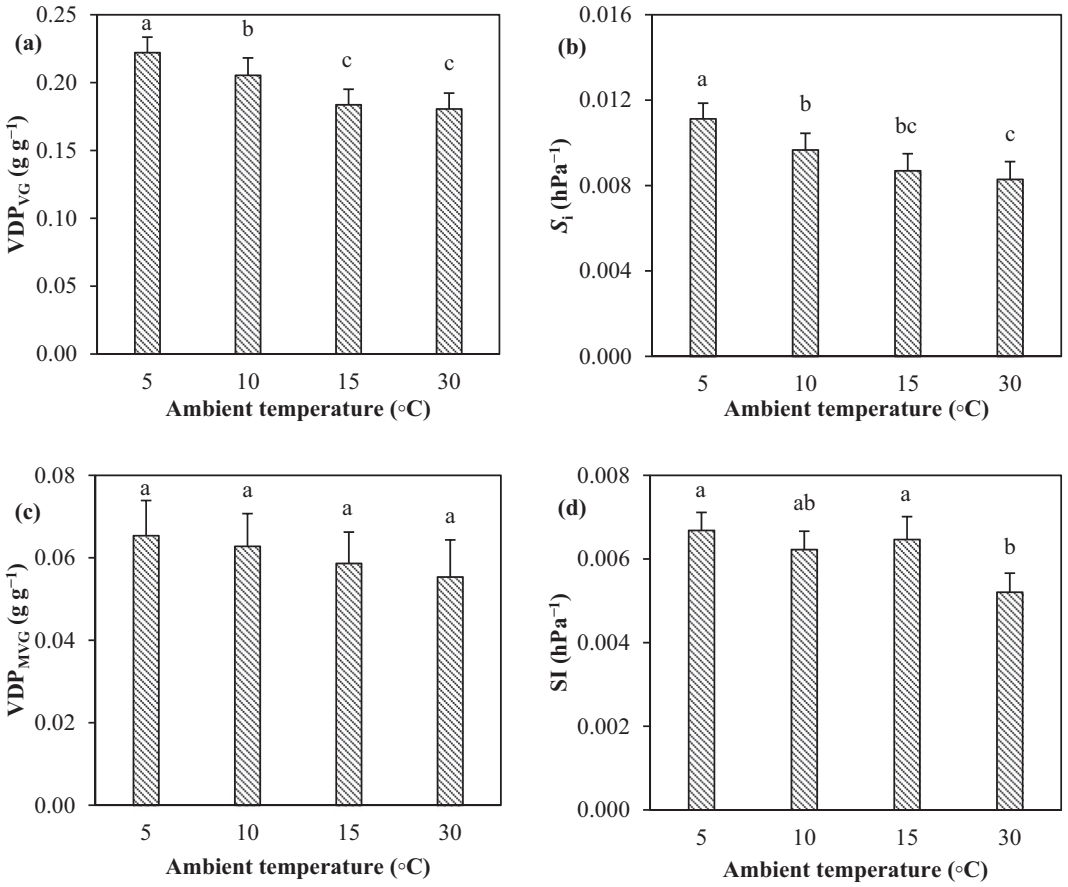

Fig. 3. Mean comparisons of the effect of ambient temperature on soil structural stability indices calculated using the van Genuchten (VG) (a and b) and modified van Genuchten (MVG) (c and d) models. (a) and (c): volume of drainable pores (VDP_{VG}, VDP_{MVG}), (b) and (d): slope at the inflection point (S_i) of HEMC and structural index (SI), respectively. For each index, columns labeled with different letters are significantly different at $P < 0.05$ (LSD); Standard errors are shown on the bars.

defined by Eq. (10), and (iii) change in the volume of entrapped air and its expansion. The pore water pressure (h) is given by Young-Laplace equation:

$$h = \frac{2\sigma \cos\gamma}{r} \tag{9}$$

where σ is the surface (interfacial) tension, γ is the soil-water contact angle and r is the effective pore radius at the location of the water/air interface menisci. Philip and de Vries (1957) stated that the decrease in h with temperature is mainly due to decrease of σ with temperature. But subsequent studies showed that the dependence of h on temperature is greater than that predicted by variation of σ. Grant and Salehzadeh (1996) assumed that in Eq. (9), r is considered independent of temperature and only σ and γ are dependent on temperature. Based on the theory of Grant and Salehzadeh (1996) and She and Sleep (1998), the contact angle (γ) would increase with an increment of temperature, but they did not provide experimental evidence for this assumption. However, the experimental data by King (1981) and Bachmann et al. (2002) indicated that γ decreases with the increase of temperature. Moreover, the results of Bachmann et al. (2002) showed that the γ decreases (1.0–8.6°) with the temperature by the rate ($\Delta\gamma/\Delta T$) of −0.03°/°C to −0.26°/°C at the range of 5–38 °C.

Large values of γ can induce water repellency to the soil (Dekker et al., 2005). On the other hand, the decrease of γ (or increase of wetting coefficient, cos γ) with ambient temperature can increase soil wettability and hydration rate. Vogelmann et al. (2013) stated that reduced rate of soil wetting and infiltration can enhance cohesion between the mineral particles. The increase of hydration rate associated with temperature rising can increase the amount of entrapped air, and therefore destruct the soil aggregates. Hence, even a small decrease in γ due to an increase in temperature might be a reason for the reduction of structural stability in the studied soils (Fig. 3).

Dexter et al. (2010) stated that the other parameter of Eq. (9), which might be affected by temperature, is the pore radius r. The electrical diffuse double layer and the presence of organic matter can influence the particle spacing. Repellent forces between the particles with negative surface charges are greater when the diffuse double layers overlap to a greater extent. The rate of decay of a diffuse double layer with distance from a particle surface is characterized by the Debye length (λ_D). At a given particle spacing, greater λ_D means more overlapping, which means more repulsion. The Debye length (λ_D) can be written in a simplified form as follows (Dexter et al., 2010):

$$\lambda_D = b\sqrt{\frac{T}{I}} \tag{10}$$

where b is a coefficient of proportionality, T (K), and I is the ionic strength of the solution. Eq. (10) shows that by increasing temperature or decreasing I, the λ_D would increase, and as a consequence the repulsive forces at constant particle spacing would be increased, and generate swelling pressure. In an unconfined system, the particles can move apart until the repulsive forces are again balanced by the water pressure in the water-filled pores, meaning that water must flow from structural pores to textural pores (Dexter et al., 2008). In a confined system (i.e., with constant volume), swelling of the textural pore space will compress the structural pore space. In both cases, the water menisci would move into smaller pores, giving rise to an increase in matric suction (Dexter et al., 2010).

We observed a decrease in soil structure stability with an increase in

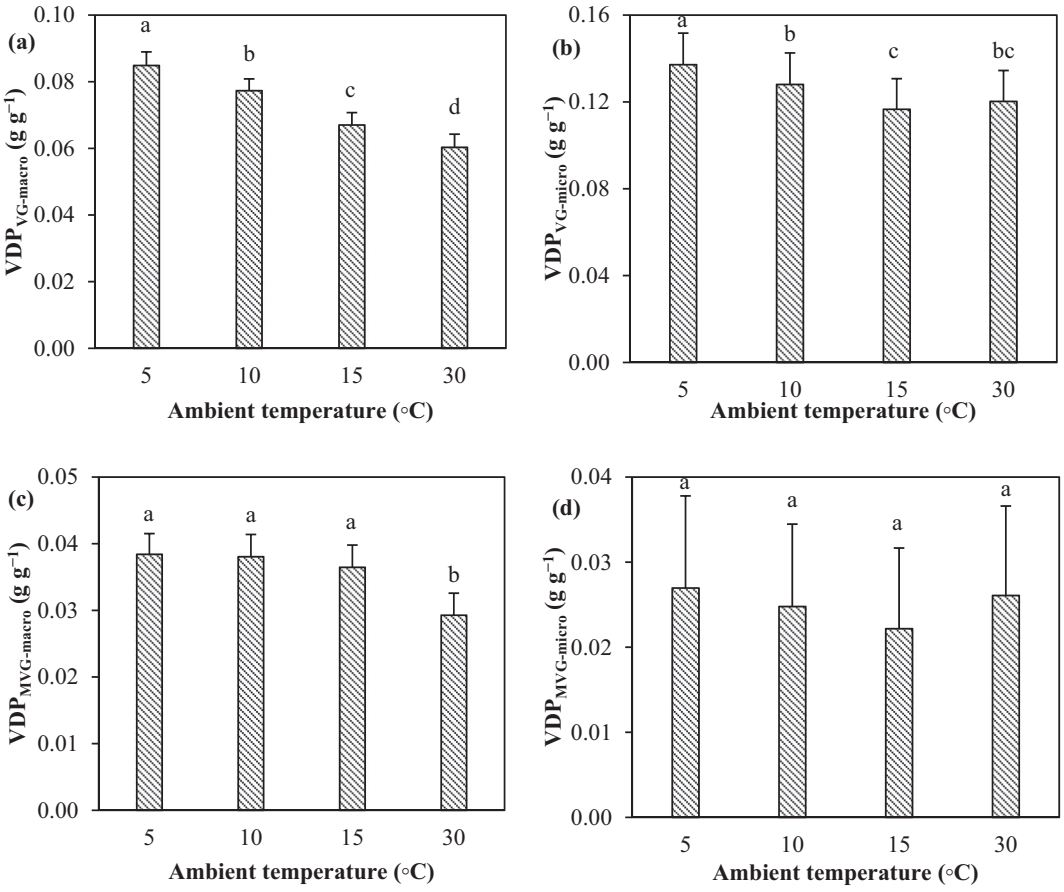

Fig. 4. Mean comparisons of the effect of ambient temperature on volumes of drainable macropores (250–1500 μm, VDP_{macro}) and micropores (60–250 μm, VDP_{micro}) calculated using (a and b) van Genuchten (VG) and (c and d) modified van Genuchten (MVG) models. (a) and (c): volume of drainable macropores ($VDP_{VG\text{-}macro}$ and $VDP_{MVG\text{-}macro}$), (b) and (d): volume of drainable micropores ($VDP_{VG\text{-}micro}$ and $VDP_{MVG\text{-}micro}$). For each index, columns labeled with different letters are significantly different at $P < 0.05$ (LSD); Standard errors are shown on the bars.

ambient temperature from 5 to 30 °C (Figs. 3 and 4). According to Eq. (10), the λ_D would increase when temperature increases or concentration of ions in the soil solution decreases. The majority of the studied soils are calcareous (CCE, mean = 36.3 kg 100 kg^{-1} and range of 10.7–63.2 kg 100 kg^{-1}, see Table 1), and solubility of calcite, aragonite and vaterite becomes higher at lower temperatures (Plummer and Busenberg, 1982). Hence, when temperature increases, the concentration of Ca^{2+} in solution decreases and as a consequence the λ_D increases, leading to rises in the repulsive forces between particles (or swelling pressure). In our experiment, soil aggregates were placed in loose state into the rings (i.e., a semi-confined system), therefore swelling pressure can trigger water flow from structural pores to textural pores and ultimately lead to compression of structural pores by textural pores. Increase of θ_{50hPa} (Fig. 2b) and VDP_{micro} at 30 °C (Fig. 4b, d) with an increase in the temperature could be associated with water flow (with low electrolyte concentration) from structural pores to textural pores and/or destruction of macropores. Decreases of VDP (especially VDP_{macro}) with increase of temperature (Fig. 4a, c) may be attributed to compression of structural pores by textural pores as induced by generated swelling pressure (Dexter et al., 2008, 2010).

We also link the decreases of soil structural stability with temperature (i) to the formation of microbubbles and their entrapment in the pore water, and (ii) the content of soil carbonates which have silt size (i.e., soils with high silt content are less stable). It is well known that all the gases are more soluble at low temperatures and less soluble at higher temperatures. The central assumption of the Peck (1960) model was that the volume of entrapped air increases with temperature but this has not been supported by the experimental data. Hopmans and Dane (1986) measured the volume of entrapped air in unsaturated soil columns and found that the volume of entrapped air decreases with the temperature elevation perhaps due to decreased solubility of gases. The theory of Dexter et al. (2010) demonstrated that temperature increase would increase the pore water suction and release of gas in the form of microbubbles from pore water. The authors measured pore water suction with a tensiometer at different steps of temperature changes and observed that an increase in temperature was always associated with a decrease in pore water suction, and vice versa. They assumed that bubbles of entrapped air will expand/contract with the increase/decrease in temperature. It was shown that the effect of increased temperature on the decrease of pore water suction is transient and may be due to expansion of entrapped air bubbles, and the decay of pressure transient could be caused by the bubbles pushing water through the pore space (Dexter et al., 2010).

Dexter (1990) found that variation of pore water suction with temperature had an inverse relationship with the clay content, and hence temperature dependence is associated with the difference in hydration of clay particles. But Dexter et al. (2010) stated that the temperature dependence of pore water suction as reported by Dexter (1990) could have been caused by the entrapped air and not by the changes in hydration rate of colloids. However, they considered that the amount of entrapped air is related to soil texture, and proportional to the clay content. Therefore, microbubbles can be generated when the temperature increases and escape from water because the solubility of all gases decreases with temperature. Microbubbles coming out from the soil solution would push the water into the pore space and contribute to destruction of macro-aggregates. This finding is in accord

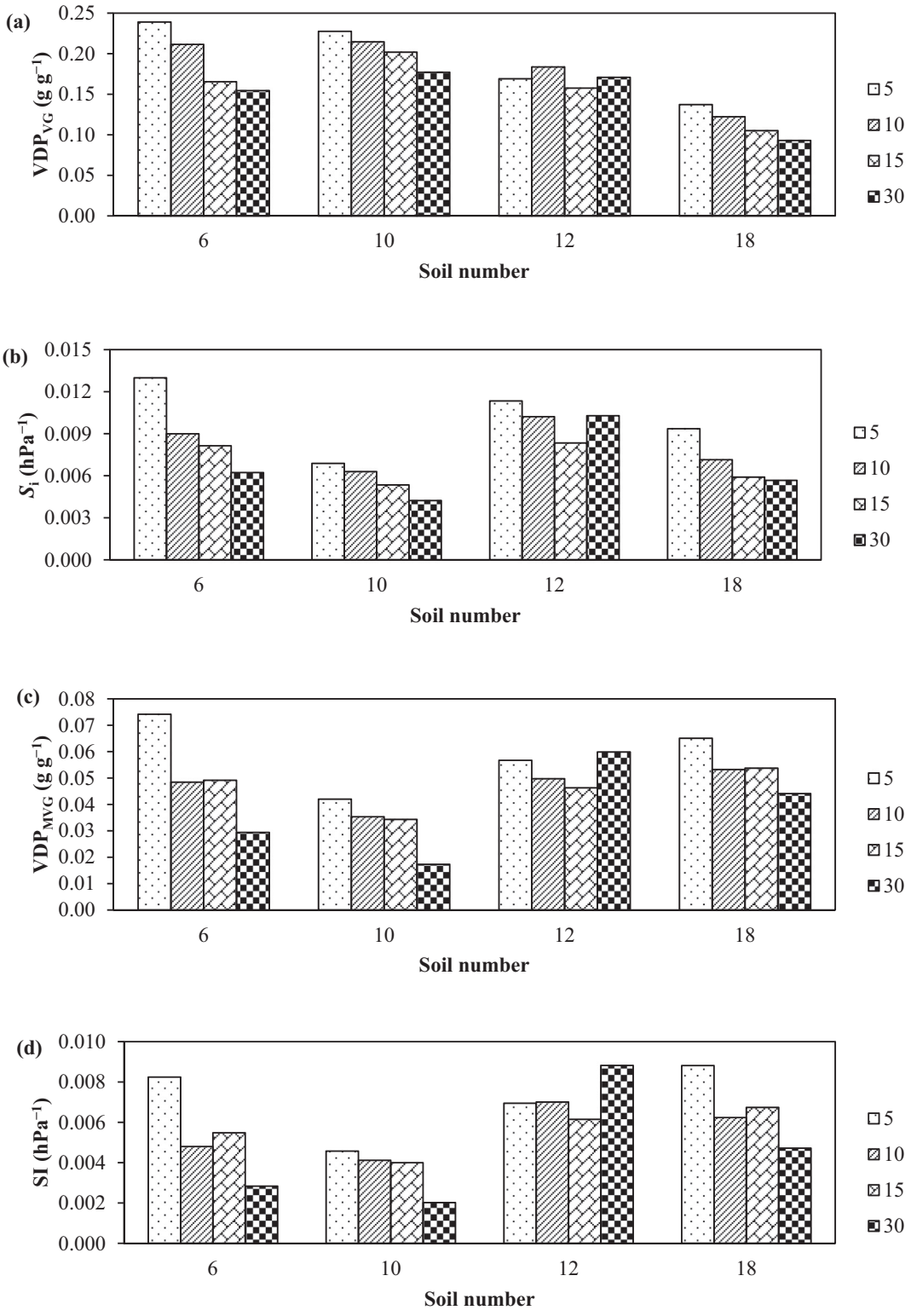

Fig. 5. Different trends in the ambient temperature effect on structural stability indices in selected soils (see Table 1 for the soil properties), (a) volume of drainable pores (VDP) calculated by the van Genuchten model (VDP$_{VG}$), (b) slope at the inflection point of HEMC (S_i) calculated by the van Genuchten model, (c) VDP calculated by the modified van Genuchten model (VDP$_{MVG}$), and (d) structural index (SI) calculated by the modified van Genuchten model.

with the hierarchical organization of soil structural elements as suggested by Tisdall and Oades (1982) and Dexter (1988). Moreover, the expansion of entrapped air with temperature can shatter and destroy the soil aggregates. Therefore, the increase of the volume and expansion of entrapped air with temperature during the fast wetting process in our experiment could be another reason for lowering structural stability of soils with mostly loam texture with an increment in temperature (Table 3).

3.5. Soil clustering results

The general trend for all the studied soils, as shown in previous

Table 4
Mean comparisons of physical and chemical properties among different soil clusters.[a]

Soil cluster	CCE	OC	Sand	Silt	Clay
	kg 100 kg^{-1}				
Cluster 1	15.6^{c}	0.74^{a}	13.4^{c}	60.2^{ab}	26.4^{ab}
Cluster 2	33.3^{b}	1.14^{a}	23.4^{b}	55.2^{b}	21.4^{b}
Cluster 3	38.9^{b}	1.68^{a}	7.7^{c}	63.2^{a}	29.1^{a}
Cluster 4	54.3^{a}	0.42^{b}	38.8^{a}	45.8^{c}	15.4^{c}

[a] OC: organic carbon, CCE: calcium carbonate equivalent. In each column, means labeled with different letters are significantly different at $P < 0.05$ (LSD).

sections, was that the soil structural stability decreased with an increase in the ambient temperature, although the trend and magnitude was soil-dependent. The values of VDP_{VG} and S_i at 5 °C were higher than those at 30 °C, except for soil number 22 with the OC of 8.9 kg 100 kg^{-1} (see Table 1). However, different trends were observed for the VDP_{VG} and S_i values at 10 and 15 °C among the studied soils (Fig. 5a, b), being dissimilar to the change in the values of VDP_{VG} and S_i. The values of VDP_{MVG} and SI at 5 °C were higher than those at 30 °C in the majority (i.e., 19 of 28) of the studied soils, although in some soils with high OC and low CCE contents, the values related to 30 °C were higher than those at 5 °C (Fig. 5c, d).

Therefore, we decided to cluster the data for better interpretation of the results. Different numbers of clusters were examined but the best results, which could be properly interpreted, were obtained by using four clusters. The results of clustering showed significant differences between the studied soils. The means of the intrinsic soil properties in the four clusters (1, 2, 3 and 4) are presented in Table 4.

Mean comparisons of the effect of temperature on θ_{2hPa}, θ_{50hPa} and $\Delta\theta_{2-50}$ in different soil clusters are shown in Fig. 6. The θ_{2hPa} had similar trends with changes in temperature in clusters 2, 3 and 4; the θ_{2hPa} increased with a decrease in temperature. However, the temperature effect on θ_{2hPa} was negligible in cluster 1 where the difference between 5 and 10 °C was not significant (Fig. 6a). Furthermore, the maximum values of θ_{50hPa} was observed at 15 °C in cluster 1, but it increased with an increment in temperature in clusters 2, 3 and 4 (Fig. 6b). The $\Delta\theta_{2-50hPa}$ of clusters 2, 3 and 4 clearly decreased with the increase in temperature but the minimum value of $\Delta\theta_{2-50hPa}$ was observed in cluster 1 at 15 °C (Fig. 6c).

Clustering showed that the structural stability indices had different trends with temperature changes in different clusters. The S_i consistently decreased as temperature increased in all four clusters (Fig. 7b). Similar trend was observed for the VDP_{VG} in clusters 2, 3 and 4 but minimum value of VDP_{VG} was determined at 15 °C in cluster 1 (Fig. 7a). A decreasing trend with an increment in temperature was observed for the VDP_{MVG} only in cluster 4 (Fig. 7c). Such a steady and consistent trend was not observed for the SI in different clusters, but the significant differences among the temperature treatments were noticeable in cluster 4 (Fig. 7d). The maximum and minimum SI values in cluster 4 were obtained at temperatures of 5 and 30 °C, respectively.

Overall results of clustering showed that aggregates were more stable at 5 °C compared to 30 °C. The effect of temperature on the structural stability indices were much visible in cluster 4 compared to clusters 1, 2 and 3 (Figs. 6 and 7) which might be due to its low OC, and high sand and CCE contents (see Table 4). Moreover, the results for cluster 1 compared to other clusters (especially cluster 4) had irregular trends in terms of water contents and structural stability indices (Figs. 6 and 7). The differences between two clusters 1 and 4 could be attributed to the differences in CCE content (Table 4). Therefore, it might be concluded that the structural stability in carbonate-rich soils (i.e., cluster 4) is more sensitive to ambient temperature changes. Carbonate dissolution may increase the electrolyte concentration of soil solution and decreases swelling pressure; on the other hand, carbonates have silt size and behavior and negatively affecting aggregate stability (Levy et al., 2003). Plummer and Busenberg (1982) reported that because

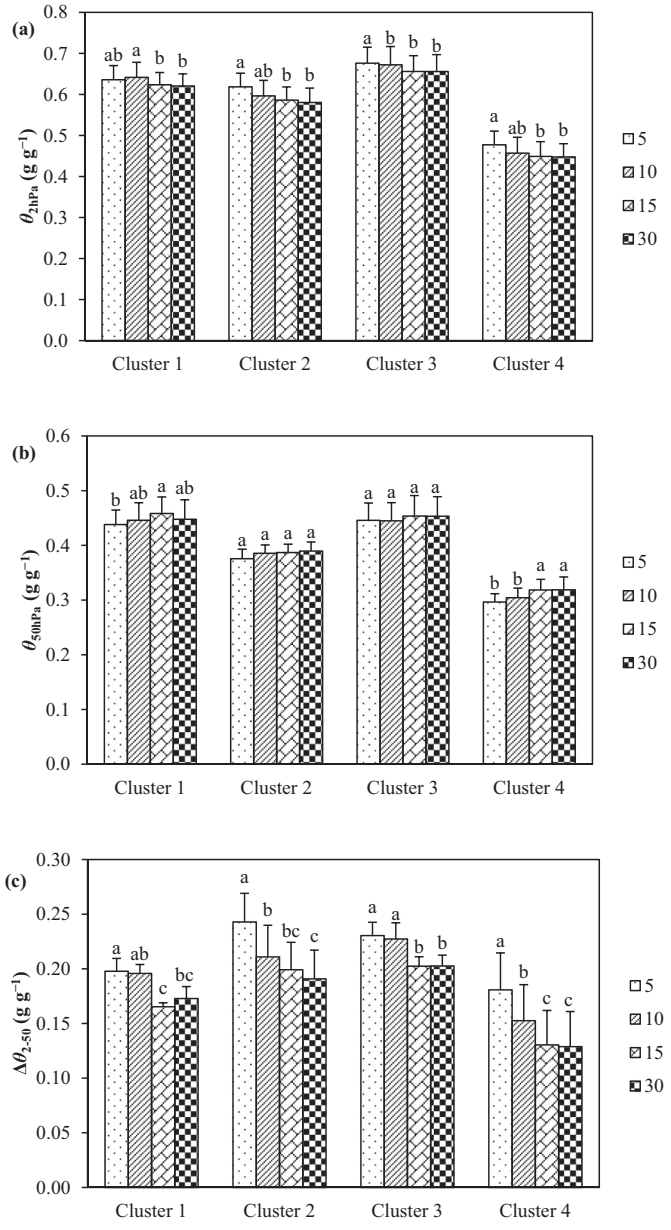

Fig. 6. Mean comparisons of (a, b) measured water contents at matric suctions (h) of 2 and 50 hPa (θ_{2hPa} and θ_{50hPa}) and (c) the total soil water released in the mentioned h range ($\Delta\theta_{2-50}$) as affected by ambient temperature in different soil clusters (see Table 3 for the soil properties of clusters). For each index in each cluster, columns labeled with different letters are significantly different at $P < 0.05$ (LSD); Standard errors are shown on the bars.

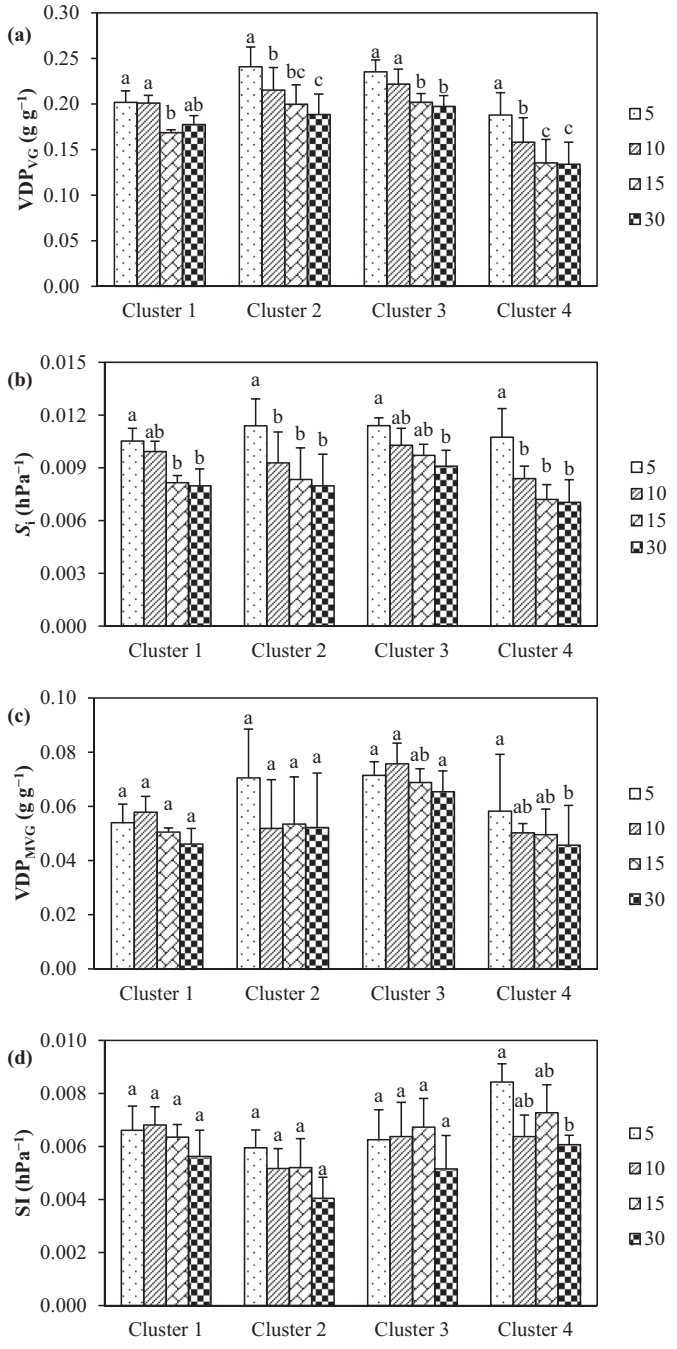

Fig. 7. Mean comparisons of the effect of ambient temperature on: (a) volume of drainable pores calculated by the van Genuchten model (VDP_{VG}), (b) slope at the inflection point of HEMC (S_i) calculated by the van Genuchten model, (c) VDP calculated by the modified van Genuchten model (VDP_{MVG}), and (d) structural index (SI) calculated by the modified van Genuchten model in different soil clusters (see Table 3 for the soil properties of clusters). For each index in each cluster, columns labeled with different letters are significantly different at $P < 0.05$ (LSD); Standard errors are shown on the bars.

solubility of calcite, aragonite and vaterite and partial pressure of carbon dioxide (P_{CO2}) are higher at low temperatures, the total Ca^{2+} concentration varies inversely with the temperature and directly with P_{CO2}.

According to Eq. (10), the Debye length and repulsive forces decrease with an increment in ions concentration. Because the soils in cluster 4 have greater CCE (Table 4), it seems that Ca^{2+} concentration is more sensitive to temperature fluctuations in this cluster. Therefore, with an increase in CCE, the effect of temperature on structure stability is more obvious. In addition, Lehrsch et al. (1991) indicated that clay particles create strong bridges between soil particles. This suspected high degree of bridging was apparently little affected by water content or repacking. Wu et al. (2017) stated that organic matter could significantly improve aggregate stability. Soils in cluster 4 have minimum means of clay and organic matter contents among the clusters (Table 4); as a result, weak clay/organic matter bridges between particles were expected in cluster 4 that confirmed the sensitivity of soil structure in this cluster to temperature changes. Soils high in CCE would have weaker structure as implied from soil shrinkage analyses of Zolfaghari et al. (2016). They showed that volume change in the structural shrinkage zone on the shrinkage curve was greater in weakly-structured calcareous soils because carbonates with low physicochemical activity would minimize resistance of aggregates against the shrinkage forces. The structural zone (in terms of moisture ratio) was curtailed in the carbonate-rich soil. The carbonate-rich soils also had low residual void ratio, indicating that carbonates might fill the micropores (Zolfaghari et al., 2016).

4. Conclusions

1) The results of this study showed that ambient temperature had a significant effect on structural stability of arid and semi-arid calcareous soils, and generally as temperature increased the structural stability decreased, mainly due to changes in pore size distribution (PSD). Macropores (250–1500 μm) markedly varied with the temperature changes but micropores (60–250 μm) did not significantly change or increased at high temperature due to intensive alteration of macropores into micropores. These findings imply that the soil structure is damaged due to loosening effects of high temperatures on inter-particles bonds which mainly destroyed the macropores. Clustering of the data showed that the temperature effect on the structural stability was greatest in carbonate-rich soils and was least in the soils rich in organic carbon.
2) Since the effect of temperature on soil structural stability is significant, it is suggested to include the effect of ambient temperature on soil structure and hydraulic properties (using pedotransfer functions) in hydrological models and soil erosion models such as LISEM (De Roo et al., 1996). This is necessary because the soil structural stability is usually determined in laboratory conditions with room temperature but the rainfall, infiltration and runoff processes would usually happen at lower temperatures in natural conditions.
3) We looked at what happens to soil PSD and structural stability when ambient temperature is changed to a single value. Yet, soil temperature shows temporal and soil-dependent variations. Further work is needed to investigate the effect of temporal variation of ambient temperature on soil structural stability and PSD.
4) It might be recommended to perform tillage operation at low temperatures (e.g., in the night) because the soil structure is more stable at low temperatures. As erosion, detachment and transport of soil particles would depend on soil structural stability, and PSD is related to aggregate/particle size distribution, the above-mentioned processes might be linked. The results could be important for forecasting the effect of global warming and climate change on soil structure and erosion, which should be considered in further studies.

List of symbols, acronyms and units

Parameter	Definition	Unit
OC	Organic carbon	$g\,kg^{-1}$
CCE	Calcium carbonate equivalent	$g\,kg^{-1}$
STVF	Surface tension-viscous flow theory	–
PSD	Pore size distribution	–
VG	van Genuchten model	–
MVG	Modified van Genuchten model	–
HEMC	High energy moisture characteristic	–
VDP	Volume of drainable pores	$g\,g^{-1}$
S_i	Slope at the inflection point of HEMC	hPa^{-1}
SI	Structural index	hPa^{-1}
SR	Stability ratio	–
h_i	Matric suction at the inflection point of HEMC	hPa
h	Matric suction	hPa
h_{modal}	Modal suction; h at the peak of C(θ)	hPa
$C(\theta)$	Specific water capacity function = $\lvert d\theta/dh \rvert$	hPa^{-1}
θ	Soil water content	$g\,g^{-1}$
θ_r	Predicted *pseudo* residual water content	$g\,g^{-1}$
θ_s	Predicted *pseudo* saturated water content	$g\,g^{-1}$
$\theta_{r\text{-observed}}$	Water content measured at h value of 50 hPa	$g\,g^{-1}$
$\theta_{s\text{-observed}}$	Water content measured at h value of 2 hPa	$g\,g^{-1}$
α	Scaling parameter of soil water retention curve	hPa^{-1}
n	Shape parameter of soil water retention curve	-
A, B and C	Quadratic terms in the modified van Genuchten model	hPa^{-2}, hPa^{-1} and $g\,g^{-1}$
θ_{2hPa}	Measured water content at h value of 2 hPa	$g\,g^{-1}$
θ_{50hPa}	Measured water content at h value of 50 hPa	$g\,g^{-1}$
$\Delta\theta_{2-50}$	Soil water released in the h range of 2–50 hPa	$g\,g^{-1}$
I	Ionic strength	$meq\,l^{-1}$
λ_D	Debye length	m
σ	Surface tension	$kg\,s^{-2}$
γ	Soil-water contact angle	degree
P_{CO2}	Partial pressure of carbon dioxide	$kg\,m^{-1}\,s^{-2}$
r	Effective pore radius	m

Acknowledgment

We would like to thank Isfahan University of Technology for the financial support of the study. Special appreciation is extended to Prof. H. Shirani of Vali-e-Asr University, Rafsanjan, Iran for his help with the cluster analysis.

References

Amezketa, E., 1999. Soil aggregate stability: a review. J. Sustain. Agric. 14 (2), 83–151.
Ariathurai, R., Arulanandan, K., 1978. Erosion rates of cohesive soils. J. Hydraul. Div. ASCE 104, 279–283.
Asgarzadeh, H., Mosaddeghi, M.R., Mahboubi, A.A., Nosrati, A., Dexter, A.R., 2010. Soil water availability for plants as quantified by conventional available water, least limiting water range and integral water capacity. Plant Soil 335, 229–244.
Bachmann, J., Horton, R., Grant, S.A., van der Ploeg, P.A., 2002. Temperature dependence of water retention curves for wettable and water-repellent soils. Soil Sci. Soc. Am. J. 66, 44–52.
Barthès, B., Roose, E., 2002. Aggregate stability as an indicator of soil susceptibility to runoff and erosion; validation at several levels. Catena 47, 133–149.
Childs, E.C., 1940. The use of soil moisture characteristics in soil studies. Soil Sci. 50 (4), 239–252.
Collis-George, N., Figueroa, B.S., 1984. The use of high energy moisture characteristic to assess soil stability. Aust. J. Soil Res. 22 (3), 349–356.
Constantz, J., 1982. Temperature dependence of unsaturated hydraulic conductivity of two soils. Soil Sci. Soc. Am. J. 46 (3), 466–470.
De Roo, A.P.J., Offermans, R.J.E., Cremers, N.H.D.T., 1996. LISEM: a single event physically-based hydrologic and soil erosion model for drainage basins. II: sensitivity analysis, validation and application. Hydrol. Process. 10, 1118–1127.
Dekker, L.W., Oostindie, K., Ritsema, C.J., 2005. Exponential increase in publications related to soil water repellency. Aust. J. Soil Res. 43, 403–441.
Demond, A.H., Roberts, P.V., 1991. Effect of interfacial forces on two–phase capillary pressure–saturation relationships. Water Resour. Res. 27, 423–437.
Dexter, A.R., 1988. Advances in characterization of soil structure. Soil Tillage Res. 11, 199–238.
Dexter, A.R., 1990. Changes in the matric potential of soil water with time after disturbance by moulding. Soil Tillage Res. 16, 35–50.
Dexter, A.R., 2004. Soil physical quality: part I. Theory, effects of soil texture, density, and organic matter, and effects on root growth. Geoderma 120 (3), 201–214.
Dexter, A.R., Czyż, E.A., Richard, G., Reszkowska, A., 2008. A user–friendly water retention function that takes account of the textural and structural pore spaces in soil. Geoderma 143, 243–253.
Dexter, A.R., Richard, G., Czyż, E.A., Giot, G., 2010. Changes in the matric potential of soil water with time and temperature. Soil Sci. 175, 320–328.
Dimoyiannis, D., 2009. Seasonal soil aggregate stability variation in relation to rainfall and temperature under Mediterranean conditions. Earth Surf. Process. Landf. 34, 860–866.
Gao, H., Shao, M., 2015. Effects of temperature changes on soil hydraulic properties. Soil Tillage Res. 153, 145–154.
Gee, G.W., Bauder, J.W., 1986. Particle size analysis. In: Klute, A. (Ed.), Method of Soil Analysis, Part 1. Physical and Mineralogical Methods, Agronomy Handbook No 9. ASA and SSSA, Madison, WI, pp. 383–411.
Grant, S.A., Bachmann, J., 2002. Effect of temperature on capillary pressure. In: Raats, P.A.C., Smiles, D., Warrick, W. (Eds.), Environmental Mechanics: Water, Mass and Energy Transfer in the Biosphere. The Philip Volume, pp. 199–212.
Grant, S.A., Salehzadeh, A., 1996. Calculation of temperature effects on wetting coefficients of porous solids and their capillary pressure functions. Water Resour. Res. 32, 261–267.
Haridasan, M., Jensen, R., 1972. Effect of temperature on pressure head-water content relationship and conductivity of two soils. Soil Sci. Soc. Am. J. 36, 703–708.
Hopmans, W.J., Dane, J.H., 1986. Temperature dependence of soil water retention curves. Soil Sci. Soc. Am. J. 50, 562–567.
Hosseini, F., Mosaddeghi, M.R., Hajabbasi, M.A., Sabzalian, M.R., 2015. Influence of tall fescue endophyte infection on structural stability as quantified by high energy moisture characteristic in a range of soils. Geoderma 249–250, 87–99.
Hosseini, F., Mosaddeghi, M.R., Hajabbasi, M.A., Sabzalian, M.R., 2016. Role of fungal endophyte of tall fescue (*Epichloë coenophiala*) on water availability, wilting point and integral energy in texturally-different soils. Agric. Water Manag. 163, 197–211.
Hosseini, F., Mosaddeghi, M.R., Hajabbasi, M.A., Mamedov, A.I., 2017. Effects of endophyte-infected and non-infected tall fescue residues on aggregate stability in four texturally different soils. Geoderma 285, 195–205.
Jacinto, A.C., Villar, M.V., Gómez-Espina, R., Ledesma, A., 2009. Adaptation of the van Genuchten expression to the effects of temperature and density for compacted bentonites. Appl. Clay Sci. 42, 575–582.
Khademi, H., Mermut, A.R., 1998. Source of palygorskite in gypsiferous aridisols and associated sediments from central Iran. Clay Miner. 33, 561–578.
King, P.M., 1981. Comparison of methods for measuring severity of water repellence of sandy soils and assessment of some factors that affect its measurement. Aust. J. Soil Res. 19, 275–285.
Lavee, H., Sarah, P., Imenson, C., 1996. Aggregate stability dynamics as affected by soil temperature and moisture regimes. Geogr. Ann. 78, 73–82.
Le Bissonnais, Y., 1996. Aggregate stability and assessment of soil crustability and erodibility: I. Theory and methodology. Eur. J. Soil Sci. 47, 425–437.
Lehrsch, G.A., Sojka, R.E., Carter, D.L., Jolley, P.M., 1991. Freezing effect on aggregate stability affected by texture, mineralogy, and organic matter. Soil Sci. Soc. Am. J. 55, 1401–1406.
Levy, G.J., Mamedov, A.I., 2002. High-energy-moisture-characteristic aggregate stability as a predictor for seal formation. Soil Sci. Soc. Am. J. 665, 1603–1609.
Levy, G.J., Smith, H., Agassi, M., 1989. Water temperature effect on hydraulic conductivity and infiltration rate of soils. S. Afr. J. Plant Soil 6, 240–244.
Levy, G.J., Mamedov, A.I., Goldstein, D., 2003. Sodicity and water quality effects on slaking of aggregates from semi-arid soils. Soil Sci. 168, 552–562.
Mamedov, A.I., Levy, G.J., 2013. High energy moisture characteristics: linking between some soil physical processes and structure stability. In: Logsdon, S., Berli, M., Horn, R. (Eds.), Quantifying and Modeling Soil Structure Dynamics. Soil Sci. Soc. Am, Madison, WI, pp. 41–74.
Mamedov, A.I., Wagner, L.E., Huang, C., Norton, L.D., Levy, G.J., 2010. Polyacrylamide effects on aggregate and structure stability of soils with different clay mineralogy. Soil Sci. Soc. Am. J. 74 (5), 1720–1732.
Mamedov, A.I., Bar-Yosef, B., Levkovich, I., Rosenberg, R., Silber, A., Fine, P., Levy, G.J., 2014. Amending soil with sludge, manure, humic acid, orthophosphate and phytic acid: effects on aggregate stability. Soil Res. 52 (4), 317–326.
Mamedov, A.I., Huang, C., Aliev, F.A., Levy, G.J., 2017. Aggregate stability and water

retention near saturation characteristics as affected by soil texture, aggregate size and polyacrylamide application. Land Degrad. Dev. 28, 543–552.
Nelson, R.E., 1982. Carbonate and gypsum. In: Buxton, D.R. (Ed.), Method of Soil Analysis, Part 2. Chemical Methods, Agronomy Handbook No. 9. ASA and SSSA, Madison, WI, pp. 181–197.
Nelson, D.W., Sommers, L.P., 1986. Total carbon, organic carbon and organic matter. In: Buxton, D.R. (Ed.), Method of Soil Analysis, Part 2. Chemical Methods, Agronomy Handbook No. 9. ASA and SSSA, Madison, WI. pp, pp. 539–579.
Noruzi Fard, F., Salehi, M.H., Khademi, H., Davoudian Dehkordi, A.R., 2010. Genesis, classification and mineralogy of soils formed on various parent materials in the north of Chaharmahal-va-Bakhtiari province. J. Water Soil 24 (4), 647–658 (in Persian with English abstract).
Peck, A.J., 1960. Change of moisture tension with temperature and air pressure, theoretical. Soil Sci. 89, 303–310.
Philip, J.R., de Vries, D.A., 1957. Moisture movement in porous material under temperature gradients. AGU Trans. 38, 222–232.
Pierson, F.B., Mulla, D.J., 1989. An improved method for measuring aggregate stability of a weakly aggregated loessial soil. Soil Sci. Soc. Am. J. 53 (6), 1825–1831.
Plummer, L.N., Busenberg, E. (Eds.), 1982. The solubilities of calcite, aragonite and vaterite in CO_2-H_2O solution between 0 and 90 °C, and the evaluation of the aqueous model for the system $CaCO_3$-CO_2-H_2O. Geochim. Cosmochim. Acta 46, 1011–1040.
Poch, R.M., Antunez, M., 2010. Aggregate development and organic matter storage in Mediterranean mountain soils. Pedosphere 20 (6), 702–710.
Pulido Moncada, M., Gabriels, D., Cornelis, W., Lobo, D., 2015. Comparing aggregate stability tests for soil physical quality indicators. Land Degrad. Dev. 26, 843–852.
Romero, E., Gens, A., Lloret, A., 2001. Temperature effects on the hydraulic behaviour of an unsaturated clay. Geotech. Geol. Eng. 19, 311–332.
Ronan, A.D., Prudic, D.E., Thodal, C.E., Constantz, J., 1998. Field study and simulation of diurnal temperature effects on infiltration and variably saturated flow beneath an ephemeral stream. Water Resour. Res. 34, 2137–2153.
Sachs, E., Pariente, S., 2017. Effect of raindrop temperatures on soil runoff and erosion in dry and wet soils. A laboratory experiment. Land Degrad. Dev. 28, 1549–1556.
SAS Institute, 2008. User's Guide. Release 9.2. SAS Inst. Inc., Cary, NC.
Saygın, S.D., Cornelis, V.M., Erpul, G., Gabriels, D., 2012. Comparison of different aggregate stability approaches for loamy sand soils. Appl. Soil Ecol. 54, 1–6.
She, H.Y., Sleep, B.E., 1998. The effect of temperature on capillary pressure-saturation relationships for air-water and perchloroethylene-water systems. Water Resour. Res. 34, 2587–2597.
Sillers, W.S., Fredlund, D.G., Zakerzadeh, N., 2001. Mathematical attributes of some soil–water characteristic curve models. Geotech. Geol. Eng. 19, 243–283.
Soil Science Society of America, 1997. Glossary of Soil Science Terms. SSSA, Madison, WI.
Tisdall, J.M., Oades, J.M., 1982. Organic matter and water-stable aggregates in soils. J. Soil Sci. 33, 141–163.
van der Drift, J.W.M., 1995. The effect of temperature change on soil structure stability. In: Zwerver, S., van Rompaey, R.S.A.R., Kok, M.T.J., Berk, M.M. (Eds.), Climate Change Research: Evaluation and Policy Implications. Studies in Environmental Science. Elsevier Science, Maastricht, The Netherlands, pp. 923–930.
van Genuchten, M.Th., 1980. A closed-form equation for predicting the hydraulic conductivity of unsaturated soils. Soil Sci. Soc. Am. J. 44 (5), 892–898.
Vogelmann, E.S., Reichert, J.M., Prevedello, J., Awe, G.O., Mataix-Solera, J., 2013. Can occurrence of soil hydrophobicity promote the increase of aggregate stability? Catena 110, 24–31.
Wraith, J.M., Or, D., 1998. Nonlinear parameter estimation using spreadsheet software. J. Nat. Resour. Life Sci. Educ. 27, 13–19.
Wu, X., Wei, Y., Wang, J., Wang, D., She, L., Wang, J., Cai, C., 2017. Effects of soil physicochemical properties on aggregate stability along a weathering gradient. Catena 156, 205–215.
Zolfaghari, Z., Mosaddeghi, M.R., Ayoubi, S., 2016. Relationships of soil shrinkage parameters and indices with intrinsic soil properties and environmental variables in calcareous soils. Geoderma 277, 23–34.